Characteristics of Extreme Rainfall Events in Northwestern Peru during the 1982-83 El Niño Period

by

R. A. Goldberg and G. Tisnado M.*
Laboratory for Extraterrestrial Physics
NASA/Goddard Space Flight Center
Greenbelt, MD 20771

and

R. A. Scofield
Satellite Applications Laboratory
NOAA/NESDIS
Washington, DC 20233

February 1987

First presented at the Chapman Conference on El Niño: An International Symposium in Guayaquil, Ecuador, October 27-31, 1986

---

*On leave from Instituto Nacional de Investigacion de Transportes (INAIT), Luis Sanchez Cerro 2100, Lima, Peru

ABSTRACT

Using rainfall data from 66 stations within the Chira-Piura Project of Northwestern Peru, we have prepared an atlas of histograms and contour maps describing the daily rainfall characteristics of the region during the El Niño period from November 1982 to June 1983. We have compared these data with those for the same 8 month intervals during the two years preceding and following the designated period. Uniquely during the El Niño period, these data often exhibit localized storms of high rainfall intensity (>100 mm/day) which may then disperse over wider areas of the region during the following 2-3 days. The region nearby and to the east of Chulucanas (5.10°S, 80.17°W) appears to be a focal point for the initiation of such events, particularly during the 1983 months of the period. Case studies for a few of the most severe events have been studied and compared with an analysis using GOES satellite cloud imagery in conjunction with upper air and surface weather maps, to arrive at a possible scenario for the cause and evolution of such events. Statistically, a high percentage of the storms are found to be multicellular with scale sizes approaching 250 km, with minimum cloud temperatures colder than -60°C, and of durations exceeding 6 hours. Such storm systems are consistent with the extreme and disastrous rainfall events observed from the ground stations. The satellite analysis has also permitted us to identify significant storms beyond the range of the ground based stations during this same time period, demonstrating the complementary value of satellite coverage for developing a more comprehensive view of the processes in effect.

INTRODUCTION

During the great El Niño episode of 1982-83, heavy and repetitive convective rainstorms were the most devastating phenomena in northwestern Peru. Normally, this region is controlled by a desert-like climate. However, during several periods within the 1982-83 El Niño episode, it was transformed into a region of extensive and raging flash floods with a great loss of life and property. It is therefore important to analyze the onset and characteristics of these storms with the intent of developing prediction capability for severe rainfalls in this area during future El Niño periods.

The work reported here was conducted under Project PREPAREN (PREcipitation PAtterns Related to El Niño), which was initiated in 1985 as a joint international program under the cosponsorship of AID/OFDA (Agency for International Development/Office of U.S. Foreign Disaster Assistance), NOAA (National Oceanic and Atmospheric Administration), NASA (National Aeronautics and Space Administration) and INAIT (Instituto Nacional de Investigacion de Transportes - Peru). PREPAREN has an objective to investigate associations between cloud patterns observed by satellite and extreme rainfall events in coastal regions of northern Peru and southern Ecuador to help develop flood alert models for these regions (e.g. Goldberg and Tisnado, 1985).

Horel and Cornejo-Garrido (1986) have considered meteorological data for this region in an effort to define possible sources for the anomalously high rainfall of the 1982-83 El Niño period. They have concentrated on monthly averages in an effort to follow trends and compare them with those of earlier El Niño and non-El Niño periods. Their work, which includes a comprehensive review of earlier studies for this region, is limited to conclusions

concerning gross features based on the monthly means, and cannot address the fine structure of the extreme rainfall events which often lasted only a few days and require daily time resolution in data for a detailed analysis.

To pursue our goal, we have analyzed daily rainfall information from 66 stations that were monitored by the Chira-Piura Special Project in northwestern Peru for the period November 1, 1982-June 30, 1983 and compared these data with GOES satellite imagery for several major rainfall events during this time interval. Rainfall from the ground stations for the same intervals up to two years preceding and following the El Niño period were also analyzed for comparison. This paper provides a description of the findings from this study and discusses their implications toward a predictive scheme.

DATA ANALYSIS AND RESULTS

1. Rainfall

The rainfall data used in this analysis were published in a series of reports, Anuario Meteorologico 1980-1983 (Chira-Piura, 1981-1984). The data from January 1984-June 1985 were provided by private communication. Figure 1A presents the geographical distribution of the rainfall stations on a map of northern Peru; table 1A lists the stations alphabetically with geographical coordinates and altitudes. Table 1B keys the stations by station numbers shown on the map in figure 1A. This region was one of the most severely affected areas during the 1982-83 El Niño episode. It was also selected because of the availability of good quality data with one day resolution as required for the analysis. Figure 1B is a contour relief map based on station altitudes, which provides a simplified but adequate

representation of the local topography. It is provided in lieu of a reliable local topographical map, mainly because it is more useful for comparison with some of the computer generated rainfall maps which follow. The contours are shown in increments of 200 m with the coastline indicated for reference.

Figure 2 displays the daily means of rainfall data from all sixty six stations, grouping them into three separate time intervals each encompassing November through June; first the average of 1980-81 and 1981-82, then 1982-83 (El Niño), and finally the average of 1983-84 and 1984-85. The July-October intervals for each year were also studied, but were found to contain insignificant rainfall regardless of year. Although these results are somewhat biased because of the nonuniform distribution in location and altitude of the contributing stations, certain features are immediately apparent. The significant rainfall during the El Niño period was far more intense and much more extensive in time than for the years preceding or following it. Furthermore, the rain intensification first consists of an increase in daily background level, and then of several large and randomly spaced intense rainfall events superimposed upon the increased background level. It is these sporadic events of intense rainfall which were responsible for the disastrous consequences of the El Niño period, mainly during 1983.

Figure 3 presents the same data partitioned into ten separate altitude domains. In this case and because of their similarity, we have grouped the two intervals preceding and following El Niño into a single average (panel 3A). The El Niño interval is shown in panel 3B. The station numbers (table 1) are also provided to indicate which and how many contribute data to each altitude region. During the non-El Niño years studied, virtually no rainfall fell at stations below 50 m altitude. Above, there was

a gradual increase in both magnitude and time interval width for rainfall occurrence. During El Niño (figure 3B) there was a strong enhancement in rainfall at the lower altitudes (up to 300 m) with more modest increases above that height. Below 300 m, the onset of rain occurred in mid-January 1983 whereas above, it began near November 1, 1982.

Once again, we can observe large sporadic events superimposed on the general background enhancements, sometimes occurring up to the highest altitudes, but more often being most dominant below 300 m in the desert area. This suggests that the large storm systems responsible for the intense rainfall events are most closely aligned with the foothills of the nearby mountains. This implication is consistent with the results which follow.

The daily data from each of the 66 stations were also entered into a sophisticated NASA scientific information and analysis system called the Pilot Climate Data System (PCDS) (Treinish, 1984; Treinish and Ray 1985; Goldberg and Tisnado, 1986). This has permitted presentation of the data in a variety of useful formats; e.g. with histograms of the total mean rainfall on a daily basis, with daily contours of rainfall of the entire region, and by surface contour maps. In fact, a daily atlas of the first two listed presentations was prepared for the El Niño period and proved extremely useful in identifying periods of extreme rainfall. From the atlas and other data, five El Niño intense rainfall events were selected for closer examination. They occurred on (1) January 22-29, 1983; (2) February 4-10, 1983; (3) March 19-27, 1983; (4) April 1-9, 1983; and (5) April 22-30, 1983. In this section, we concentrate on event (4), since this typifies the general properties of all periods examined. In the next section dealing with satellite results, data from all five intervals are used to obtain the results provided.

Six days of event (4) data (April 3-8) are displayed in the six panels of figure 4. The data are shown by individual station, with coding used to designate daily rainfall in millimeters (mm). The cluster of 4 key rainfall stations, Chulucanas (9), San Pedro (27), Morropon (10), and Santo Domingo (24); as well as an outline of the coastline are depicted for reference. The sequence begins with rain storms (>50mm) over the desert regions on April 3 followed by increased storm magnitude and number on April 4. There is a definite eastward movement toward the mountains. On April 5, we find the development of a large storm (>100mm) centered to the northeast of Chulucanas (9) near Santo Domingo (24). Over the next three days, the rain is observed to spread westward and become more uniform over the desert plain before subsiding.

The same data are depicted as contour maps in figure 5. Here each panel represents rainfall intensity as a function of geographic coordinates. The contours have been generated from a uniform grid, which was produced using nearby (to each grid point) station values normalized and weighted by their inverse distance squared to the appropriate grid point. In this case, to minimize washout of the minor features, only the three nearest stations to each grid point were used in the analysis. Contours shown are usually 10 mm of daily rainfall apart. From the sequence, we once again observe rainfall development in the low altitude regions on April 3 and 4, followed by the intense storm to the northeast of Chulucanas on April 5, which is even more apparent than in figure 4C. The contour representation of the gradual rainfall spreading to the west over the desert regions and the ensuing abatement is depicted in figures 5D-5F.

The developing scenario from this preliminary analysis is then the following. A convective rain system appears near the coast and moves eastward for 1-2 days. Upon orographic interaction

with the Andean foothills, a much larger convective storm system appears and intensifies, before spreading northwestward and/or southwestward back toward the coastline over the lowland desert regions. The next sections will provide additional evidence to justify and expand this hypothesis.

2. Satellite Cloud Studies

Here we examine the characteristics of heavy precipitation in northern Peru during the 1983 El Niño period from satellite observed cloud structure. The data sources include GOES infrared (IR), enhanced IR (EIR) and visible (VIS) imagery (every 1/2-1 hour) (cf. Clark, 1983), EIR movie loops, the contour rainfall maps discussed in the last section, and surface/700 mb/500 mb/250 mb analyses. Figure 6 provides an example of an unenhanced and EIR picture of a heavy rainfall producing convective system over northwestern Peru.

For the period studied, four basic classifications of heavy precipitation-producing, convective systems have been identified over northwestern Peru. They are mesoscale convective complex (MCC) (cf. Maddox, 1980), multi-clustered circular (MC), multi-clustered linear (ML), and single clustered (SC). Satellite photographic examples of each type system are shown in figure 7.

Using a methodology similar to that applied by Fleming et al (1984) and Fleming and Spayd (1986) for regions of the eastern and western United States, and by Scofield (1986) over China, it has been possible to analyze the five intervals discussed in the last section and arrive at the results presented in this section. This methodology classifies each type of convective system producing heavy rainfall into the above categories, and further classifies each event by time of year, time of day of maximum rainfall and finally, the time duration of each event. The El

Niño intense rainfall periods used in this analysis are once again: (1) January 22-29, 1983; (2) February 4-10, 1983; (3) March 19-27, 1983; (4) April 1-9, 1983; and (5) April 22-30, 1983. Statistics determined from a study of convective cloud systems in each of the periods have been assembled to produce the results which follow.

Seventy two rainfall producing convective systems were observed during the five intervals named above. These are listed according to their cluster classification in table 2. We find that 17% were MCC's. 79% were multi-clustered (MC or ML), and only 4% were single clustered (SC). We note here that the satellite data covers an area somewhat larger but inclusive of the Chira-Piura region. This permitted us to identify storm systems in northwestern Peru, in southern Ecuador and over the coastal Pacific during each period.

Table 3 shows the time of maximum intensity for each rainfall producing convective system. The large MCC's are mainly local evening and nighttime events, whereas the ML's and MC's are observed to peak either at night or in the late afternoon. We have also compared the number of rainfall convective systems in each category to their minimum IR temperatures (table 4). All of the MCC's and 81% of the ML's and MC's had tops colder than $-60^{o}C$. The cold cloud tops are indicative of high altitude penetration for these convective systems, which in turn is a measure of their convective strength and rainfall intensity; e.g., Negri and Adler (1981) have shown that the satellite defined tops of thunderstorms correlate well with the location and intensity of radar echoes from the rainfall itself.

The meteorological scale size of each rainfall system was also measured (table 5). All of the MCC's and 67% of the multi-cluster systems were meso-β (~25 to ~250 km). The balance of the

multi-cluster systems and the three SC's were meso-γ (~2.5 to ~25 km). Comparison of the heavy rainfall producing systems to their duration is provided in table 6. For the MCC's, all lasted more than 6 hours with 50% operating in excess of 12 hours. For the multicluster systems, the duration for the highest percentage of storms (54%) was between 3 and 6 hours. The large scale sizes coupled with long duration for a high percentage of the storms is consistent with the high daily rainfalls seen for many of the ground stations during the El Niño periods under study.

We have also identified the number of rainfall systems associated with mergers. This is important because such established heavy rainfall events can be amplified and sustained for longer periods of time through the merger action. An example of two thunderstorm clusters (A and B) merging over northern Peru and southern Ecuador is shown in the three plate sequence of figure 8. The sequence of IR and EIR photographs are for April 3, 1983 at 0030 GMT (1), 0300 GMT (2) and 0630 GMT (3). In panel 3, the large merged cluster indicated by "M" is a good example of an MCC. In our study, 10 mergers of this type were identified with 8 being associated with MCC's; i.e. 67% of the MCC's were associated with mergers.

Since most of the storms were of large meteorological scale size (meso-β) and penetrated to high altitudes ($< -60^{o}C$), this implies intensive convection and rainfall. The duration of the storms was also abnormally high, the longest of which were induced by merger of smaller systems. These results, coupled with our knowledge that most storms reached maximum intensity during the evening and nighttime hours, suggest convective interactions among convective outflow boundaries, low level jets, radiational cooling of cloud tops and orographic effects from the Andes and their foothills.

DISCUSSION

The rainfall data have indicated a repetitive pattern whereby during each selected period of the El Niño 1982-83 episode, the convective rain activity developed near the coastal region of northwestern Peru. It then moved inland (eastward) depositing rain over the desert areas through scattered storms before approaching the Andean foothills. There, the storms were rejuvinated through convective activity involving orographic effects and other processes mentioned at the end of the previous section, leading to the development of large storm systems (some becoming of MCC magnitude) which then spread back across the desert plains to the northwest and/or southwest before dissipating. The origin of the initial coastal convection will be addressed later in this section. For now we wish to concentrate on some specific characteristics of the rainfall development.

Figures 4C and 5C have both been used to isolate a large storm to the northeast of Chulucanas (9) at Santo Domingo (24) on April 5, 1983. By April 6 it had grown to cover the entire region encompassing Morropon (10), San Pedro (27) and of course, Chulucanas. This storm was identified as an intense convective system which developed upon interaction of the eastward moving rain system with the Andean foothills. Furthermore, our contour map atlas showed this large storm development near Chulucanas to be a repetitive process which reoccurred numerous times during the El Niño period. Rainfall here often approached or exceeded 100 mm/day, e.g. as depicted for March-April, 1983 at Chulucanas (figure 9). The unique 1983 El Niño rainfall characteristics for this region can also be demonstrated by comparing contours of annual rainfall for 1983 with the annual mean for non-El Niño years (figure 10; Mugica, pvt. communication). During a typical year, the mean annual rainfall near Chulucanas is approximately

250 mm. However, during 1983, this rose more than an order of magnitude to a value exceeding 4000 mm. Furthermore, the contour isohyets, which normally run parallel with the orographic relief, were now found to be distorted with a focal point centered near Chulucanas. From figure 9, we find that many of the local storms near Chulucanas during El Niño produced a daily rainfall of 30 to 50% the annual value for other years.

The terrain structure in the Chulucanas region offers a possible explanation for the uniqueness of this area as a rainfall focal point. Approximately 20 km east of Chulucanas lies a mountain ridge running from the northwest to the southeast to form a low wall which has a local maximum altitude at Cerro Peña Blanca peak (1824 m), illustrated in figure 11. Behind this leading edge are higher mountains, some approaching 4000 m. Perpendicular to this mountain chain are a series of ridges which descend down to the plains. Two of these reach out toward either side of Chulucanas to define a horseshoe valley (cf. figure 11), naturally shaped to catch moisture moving to the northeast (perpendicular to the coastline) and funnel it to higher altitudes where convective action can occur. The two ridges on either side of Chulucanas are the most westward and highest of any in the chain, making the Chulucanas region the most likely area to intercept moisture moving inland from the coast near Piura. This idea is further substantiated by our finding from the rainfall atlas that the two stations San Pedro and Santo Domingo, which are to the northeast beyond the valley entrance, often exhibit the initial intensification of storms in this region.

The origin of the eastward moving rain systems from the coast in northern Peru is a complex problem under current study and to be presented elsewhere. Here we briefly present our ideas on the subject to complete the scenario discussed above. The five 1983 heavy rainfall events selected for analysis in the previous

section were not chosen solely by rainfall characteristics. From GOES VIS data, we have also identified a multistage process depicted by cloud patterns which preceded and then characterized each period studied. These plus the heavy rainfall sequence were used to make the event selections.

As indicated from GOES photographs and other meteorological data, each major rainfall event was first accompanied by the intensification of the large quasi-stationary anticyclonic system in the South Pacific. This then drove lower tropospheric wind surges up along the coast of Peru, since the flow could not spread eastward because of the barrier offered by the Andes mountain chain. Along the central coast, the surge flow was apparently channeled parallel to the Andes and coastline in association with low level convective cloud lines or cloud streets; these cloud features represent regions of maximum moisture concentrations. The Intertropical Convergence Zone (ITCZ), which during El Niño is displaced several degrees southward to southern Ecuador, provided an east-west (E-W) boundary for the northward extent of the surge movement. This is consistent with the observation that during non-El Niño years, the ITCZ is located further north, as are the convective thunderstorm regions. Next, the warm El Niño ocean current caused enhanced evaporation to produce a warmer and more moist atmosphere in the lower troposphere along the north Peruvian coast. Other mechanisms, such as differential heating (Atlas et al., 1983), may also have been operative. Hence in northern Peru, the inversional stratifications, which are the normal condition during non-El Niño years, were broken down and a local environment was created which was favorable for the development of deep convection.

Evidence for flow surges is present in much earlier studies. For example, Morgan (1965) considered surges of the Antarctic high in

Evidence for flow surges is present in much earlier studies. For example, Morgan (1965) considered surges of the Antarctic high in relation to the hurricane seasons of 1962 and 1963 in the North Atlantic. He attempted to correlate the incidence of tropical storm development in the eastern North Atlantic in 1962 and 1963 with intense Antarctic air outbreaks penetrating deeply into the tropical regions of the South Atlantic.

A sample of the convective line flow is shown in figure 12A for April 3, 1983. When such cloud lines branch together or intersect, as was the case off the north coast of Peru during El Niño, convective activity at the merger points is highly intensified, leading to the development of rain bands with a drift flow normal to the line clouds at their point of merger (figure 12B). This activation is not uncommon and is, for example, somewhat analagous to what happened on 15 June 1977, when two convective cloud lines (L-H and S-H) intersected near Houston, Texas (at H in figure 13); the result was 380 mm of rain and severe flash flooding. It has been documented (Scofield and Oliver, 1977) that merging convective cloud lines usually increase the rainfall rate in the vicinity of the merger. A theoretical description for the onset of rain bands perpendicular to cloud streets near their point of convergence has recently been described by Xu (1986).

Convective cloud lines of the type illustrated in figure 12 have been observed by our study mostly during the El Niño period of 1982-83. This may imply that either such cloud streets cannot easily form or cannot be observed at other times. The streets normally occur off the central and north-central coastline of Peru, alongside some of the highest mountains in the Andean wall. Arkin et al. (1983) and Rasmusson and Arkin (1985) have already shown an anomalous behavior of winds crossing this region of the Andes during the El Niño period. They found a major, tri-monthly

1983. Moreover, we have observed a large easterly wind field at 700 mb (e.g., figure 14A) along with northward surface winds parallel to the coast (e.g., figure 14B) during the early stages of each event studied. Normally, the 700 mb wind structure across this region is either in some other direction, or contains much weaker easterlies. Furthermore, the mid-level winds subsided or disappeared after 2-3 days into each event. These observations would lead us to conclude that interaction of the mid-level easterly flow with the northbound low level surges enhances the prospect for cloud street formation, possibly through windshear and/or Lee wave action. Of course, if the 700 mb easterlies are responsible for making the convective line flow visible, then the surge transport from South Atlantic highs could occur at any time, implying that the ITCZ southern boundary may be one of the primary causes for the location of convective action induced by cloud street mergers.

CONCLUSIONS

We have analyzed the daily characteristics of rainfall in northwestern Peru during the 1982-1983 El Niño period and compared these results with data from prior and succeeding years. Analysis of these ground station data showed the major impact of El Niño rainfall intensification to occur in the coastal plain below 300 m altitude. Here, the principal activity did not begin until January 1983 and concluded by June 1983. At higher altitudes, a rainfall enhancement above non-El Niño values also occurred, with the rainy season extending over the entire interval from October 1982 through June 1983. In both the high and low altitude station data, there was a general increase in daily background levels, but also and perhaps more importantly, sudden and repetitive bursts of extreme rainfall events. These

bursts, which were primarily responsible for the disastrous flooding that followed, may be related to convective phenomena quite different than that responsible for the increase in general background levels. For example, from analysis of monthly means for various meteorological data, Horel and Cornejo-Garrido (1986) have suggested a mechanism for the latter involving circulation from the Amazon Basin, which is quite different from that which we have offered here.

By studying the daily rainfall through a network of 66 stations in northwestern Peru, it has been possible to track the convective systems inland from the coast, monitor their amplification upon convective interaction at the Andean foothills, and observe the ensuing dispersion and dissipation over the entire or partial coastal plain. Five of the most pronounced events were selected for this study, with each exhibiting similar features. From analysis of GOES satellite data for each of the selected events it has been possible to arrive at conclusions regarding the convective storm characteristics during such periods. They are found to be mainly of the MCC or multicluster variety, usually quite large (meso-β scale), of high altitude with cloudtop temperatures at peak development colder than $-60^{o}C$. The storms also show a tendency for evening and nighttime growth and maturation and are found to be of long duration, many lasting in excess of 6 hours and some in excess of 12 hours. These findings help account for the disastrous consequences induced by their occurrence. The long storm lifetime is caused in part by merging of cells and/or storm systems, which was found to occur in 10 of the 72 storms identified, and which can also lead to strong convective enhancements making additional contributions to the heavy rainfall.

Many of the general storm characteristics listed above make Peruvian convection in satellite imagery quite amenable to analysis. The most important features of the rainfall systems are that they are somewhat localized, of long duration, reach cold cloudtop temperatures, and are often large. In addition there are available rainfall data from the ground station network of adequate quality to calibrate and verify the remote sensing techniques. These include manual and interactive convective precipitation estimation techniques (Scofield, 1987) and totally objective techniques (Griffith et al., 1978). Barrett (1985) has developed an approach making use of an assortment of the above. Any or all of these approaches could be fine tuned and calibrated for use in the Peruvian and Ecuadorian sectors.

Another benefit of the satellite data has been to extend the domain of analysis beyond the region encompassed by the ground station network. Although the satellite data cannot teach us the characteristics of rainfall with the same resolution provided by the station network, we have learned that many of the storm systems were of much larger extent than, or actually located outside of the Chira-Piura area, sometimes reaching westward into the Pacific and northward into southern Ecuador. Future plans include detailed study of daily data acquired from stations in these regions, to better understand the processes involved. The value of working with daily data sets (as opposed to e.g., monthly averages) has been well demonstrated in the analysis presented here.

Finally, we have suggested a possible mechanism to explain the source of moisture and convective processes for the intermittent, large and disastrous rainfall events which occurred in northwestern Peru during the 1982-83 El Niño period. The large anticyclonic system in the South Pacific first generated lower tropospheric air surges which then traveled northward parallel to

the Peruvian coast, guided in part by the Andean mountain chain. These surges appeared to be associated with convective lines which merged near the northern Peruvian coast at the southern E-W boundary of the ITCZ, which is displaced to latitudes of southern Ecuador and northern Peru during each El Niño period. The convective action caused by these cloud line mergers along with heating from the warm El Niño ocean current then produced outflow boundaries which moved eastward. Interaction between the outflow boundaries, low level jets, radiational cooling of cloud tops and orographic effects produced large multicluster and MCC type systems. These systems were responsible for the devastating flash floods in the coastal plain regions. This repetitive pattern offers prospects for development of a predictive scheme to provide an alert of 1-3 days advance warning for the occurrence of these severe storms during future El Niño events.

The occurrence of easterly flow across the Andes in central and southern Peru, coupled with the observation of long cloud streets parallel to the coast, was also found to be nearly unique to the El Niño period. This implies that the easterly flow may contribute to the formation of such cloud streets, which were not observed during the non-El Niño periods covered by this study. The relationship of the mid-level easterly flow to this type of cloud street formation and convective development in northwestern Peru requires additional study. Further analysis is now in progress to attempt to answer this and some of the other intriguing questions opened by this research.

ACKNOWLEDGEMENTS

We thank P. Krumpe (OFDA, Washington) and M. Hirsh (OFDA, AID Mission, Peru) for their interest and support of this research. We are further appreciative to Drs. L. Steyaert (NOAA Program Manager) and J. Hock (Director, Assessment and Information Services Center, NOAA) for their support and assistance to gain access to many of the necessary NOAA facilities, equipment, and data used in this work. G. Dunlap and J. Shadid (NOAA) provided the satellite pictures shown here. We are indebted to Dr. J. Green (Director) and L. Treinish of the NASA/Space Science Data Center for their backing and assistance in implementing the Pilot Climate Data System for this study. We also recognize the detailed and, sometimes tedious, programming and data analysis provided by P. Twigg and D. Lessler. We appreciate the continued strong support for this program given by Dr. S. Cajja (Director, Instituto Nacional de Investigacion de Transportes). Our thanks also go to A. Joo Chang and M. Otero (of the Proyecto Especial Chira-Piura) for providing the critical rainfall data used herein, and to Professor R. Mugica (Univ. of Piura) for providing summary rainfall contour maps and several valuable scientific discussions.

REFERENCES

Arkin, P. A., J. D. Kopman, and R. W. Reynolds, 1982-1983 El Niño/Southern Oscillation Event Quick Look Atlas. U. S. Dept. of Commerce, NOAA/National Weather Service, National Meteorological Center, Washington, DC, 1983.

Atlas, D., S. Chou, and W. P. Byerly, "The influence of coastal-shape on winter mesoscale air-sea interaction", Mon. Wea. Rev., 111, 245-252, 1983.

Barrett, E. C., AgRISTARS Stage 5: The Bristol/NOAA Interactive Scheme for Satellite-Improved Rainfall Monitoring: Operational and Training Considerations. Final Report (Part 1) to the U. S. Dept. of Commerce, Cooperative Agreement No. NA-85-AA-H-RA010, Remote Sensing Unit, University of Bristol, UK, 1985.

Chira-Piura Reports (4), Anuario Meteorologico Año 1980, 1981, 1982 and 1983. All published by the Division de Hidrometeorologia, Direccion Ejecutiva del Proyecto Especial Chira-Piura, Peru. Dates of Reports are Nov. 1981, Dec. 1982, Sept. 1983 and Sept. 1984, respectively. 1981-1984.

Clark, J. D. (Editor), The GOES User's Guide. U. S. Dept. of Commerce, NOAA/NESDIS, Washington, DC, June, 1983.

Fleming, E. L., and L. E. Spayd, Jr., "Characteristics of Western Region flash flood events in GOES imagery and convectional data." NOAA Technical Memorandum NESDIS 13, U. S. Dept. of Commerce, NOAA/NESDIS, Washington, DC, 1986.

Fleming, E. L., E. L. Spayd, Jr., and R. A. Scofield, "Characteristics of Eastern Region flash flood events in GOES imagery." Proceedings of the 10th Conference on Weather Forecasting and Analysis, June 25-28, 1984, Clearwater Beach, FL, pp. 409-417, 1984.

Goldberg, R. A. and G. Tisnado M., "Andean Lee waves on the western slopes during El Niño." Proceedings of the Conference on Ciencia, Tecnologia y Agresion Ambiental: El Fenomeno El Niño, pp. 229-239, June 4-9, 1984, Lima, Peru, 1985.

Goldberg, R. A., and G. Tisnado M., "Analysis of rainfall over Northern Peru during El Niño--A PCDS application." Proceedings of the Second Pilot Climate Data System Workshop, January 29-30, 1986, NASA/Goddard Space Flight Center, Greenbelt, MD, 1986.

Griffith, C. G., W. L. Woodley, P. G. Grube, D. W. Martin, J. Stout, and D. N. Sikdar, "Rain estimation from geosynchronous satellite imagery - visible and infrared studies." Mon. Wea. Rev., 106, 1153-1171, 1978.

Horel, J. D. and A. G. Cornejo-Garrido, "Convection along the coast of Northern Peru during 1983: Spatial and temporal variation of clouds and rainfall." Mon. Wea. Rev., 114, 2091-2105, 1986.

Maddox, R. A., "Mesoscale convective processes." Bull. Am. Met. Soc., 61, 1374-1387, 1980.

Morgan, M. R., "Outbreaks of Antarctic air in relation to the hurricane seasons of 1962 and 1963 in the North Atlantic." Canadian Meteorological Branch Circular 4234, Tech. No. 571, May 17, 1965.

Negri, A. and R. Adler, "Relation of satellite-based thunderstorm intensity to radar estimated rainfall." J. Appl. Met., 20, 66-78, 1981.

Rasmusson, E. M. and P. A. Arkin, "Interannual climate variability over South America and the Pacific associated with El Niño episodes." Proceedings of the Conference on Ciencia, Tecnologia y Agresion Ambiental; El Fenomeno El Niño, pp. 179-206, June 4-9, 1984, Lima, Peru, 1985.

Scofield, R. A., "The NESDIS operational convective precipitation estimation technique." Mon. Wea. Rev., 115, 1987 (In Press).

Scofield, R. A., "Satellite characteristics of heavy rainfall events over China between June 23 and September 21, 1985." Proceedings of the 11th Conference on Weather Forecasting and Analysis, June 17-20, 1986, Kansas City, MO, pp. 321-329, 1986.

Scofield, R. A., and V. J. Oliver, "A scheme for estimating convective rainfall from satellite imagery." NOAA/NESDIS Technical Memorandum 86, U. S. Dept. of Commerce, NOAA, Washington, DC, 1977.

Treinish, L. A., "A general scientific information system to support the study of climate-related data." NASA Technical Memorandum 86152, NASA/Goddard Space Flight Center, Greenbelt, MD, September, 1984.

Treinish, L. A. and S. N. Ray, "An interactive information system to support climate research." Proceedings of the First International Conference on Interactive Information and Processing Systems for Meteorology, Oceanography, and Hydrology, January 7-11, Los Angeles, CA, pub. by the American Meteorological Society, Boston, MA, 1985.

Xu, Q., "Conditional symmetric instability and mesoscale rain bands", Quart. J. Met. Soc., 186, 315-334, 1986.

Table 1A. Alphabetical listing of rainfall stations with their coordinates.

Station Name	Station Number	Latitude (Deg.)	Longitude (Deg.)	Altitude (Meters)
ALTAMIZA	29	-5.07	-79.73	2600
ANIA	17	-4.85	-79.48	2450
ARANZA	16	-4.85	-79.58	1300
ARDILLA	40	-4.52	-80.43	150
ARENALES	8	-4.92	-79.85	3010
ARRENDAMIENTOS	57	-4.83	-79.90	3010
AUL	42	-4.55	-79.70	640
AYABACA	2	-4.63	-79.72	2700
BARRIOS	33	-5.28	-79.70	310
BERNAL	36	-5.47	-80.73	32
BIGOTE	34	-5.33	-79.78	200
CANCHAQUE	35	-5.37	-79.60	1200
CHALACO	25	-5.03	-79.80	2250
CHIGNIA	60	-5.60	-79.70	360
CHILACO	3	-4.70	-80.50	90
CHULUCANAS	9	-5.10	-80.17	95
CHUSIS	37	-5.52	-80.82	12
CIRUELO	64	-4.30	-80.15	202
CORPAC	15	-5.20	-80.62	49
ESPINDOLA	49	-4.63	-79.50	2300
FRIAS	20	-4.93	-79.93	1700
HUANCABAMBA	68	-5.23	-79.43	1052
HUAR HUAR	62	-5.08	-79.47	3150
HUARA DE VERAS	47	-4.58	-79.57	1680
HUARMACA	14	-5.57	-79.52	2100
JILILI	46	-4.58	-79.80	1330
LA ESPERANZA	7	-4.92	-81.07	12
LA TINA	1	-4.40	-79.95	427
LAGARTERA	54	-4.73	-80.07	307
LAGUNA RAMON	59	-5.55	-80.67	9
LAGUNA SECA	19	-4.88	-79.48	2450
LANCONES	45	-4.57	-80.47	110
LAS LOMAS	66	-4.65	-80.25	265
LOS ALISOS	21	-4.97	-79.53	2150
MALLARES	6	-4.85	-80.73	45
MIRAFLORES	11	-5.17	-80.62	30
MONTEGRANDE	13	-5.35	-80.72	27
MONTERO	48	-4.63	-79.83	1070
MORROPON	10	-5.18	-79.98	140
NANGAY DE MATALACAS	18	-4.87	-79.77	2100
OLLEROS	53	-4.70	-79.65	1360
PACAYPAMPA	23	-5.00	-79.67	1960
PAITA	67	-5.08	-81.13	6
PALO BLANCO	28	-5.05	-79.63	2800
PALTASHACO	30	-5.12	-79.87	900
PANANGA	43	-4.55	-80.88	450

PARAJE GRANDE	65	-4.63	-79.92	1500
PASAPAMPA	31	-5.12	-79.60	2410
PICO DE LORO	41	-4.53	-79.87	1325
PIRGA	61	-5.67	-79.62	1510
PUENTE INTERNACIONAL	63	-4.38	-79.95	408
SAN JOAQUIN	32	-5.13	-80.35	100
SAN MIGUEL	12	-5.23	-80.68	29
SAN PEDRO	27	-5.08	-80.03	254
SANTO DOMINGO	24	-5.03	-79.87	1475
SAPILLICA	56	-4.78	-79.98	1446
SAUSAL DE CULUCAN	4	-4.75	-79.77	980
SICCHEZ	44	-4.57	-79.77	1435
SUYO	39	-4.50	-80.00	250
TACALPO	50	-4.65	-79.60	2010
TALANEO	26	-5.05	-79.55	3430
TAPAL	55	-4.77	-79.55	1890
TEJEDORES	5	-4.75	-80.25	230
TIPULCO	52	-4.70	-79.57	2600
VADO GRANDE	38	-4.45	-79.60	900
VIRREY	58	-5.53	-79.98	230

Table 1B. Listing of rainfall stations by number code.

Station Number	Station Name	Station Number	Station Name
1	LA TINA	35	CANCHAQUE
2	AYABACA	36	BERNAL
3	CHILACO	37	CHUSIS
4	SAUSAL DE CULUCAN	38	VADO GRANDE
5	TEJEDORES	39	SUYO
6	MALLARES	40	ARDILLA
7	LA ESPERANZA	41	PICO DE LORO
8	ARENALES	42	AUL
9	CHULUCANAS	43	PANANGA
10	MORROPON	44	SICCHEZ
11	MIRAFLORES	45	LANCONES
12	SAN MIGUEL	46	JILILI
13	MONTEGRANDE	47	HUARA DE VERAS
14	HUARMACA	48	MONTERO
15	CORPAC	49	ESPINDOLA
16	ARANZA	50	TACALPO
17	ANIA	52	TIPULCO
18	NANGAY DE MATALACAS	53	OLLEROS
19	LAGUNA SECA	54	LAGARTERA
20	FRIAS	55	TAPAL
21	LOS ALISOS	56	SAPILLICA
23	PACAYPAMPA	57	ARRENDAMIENTOS
24	SANTO DOMINGO	58	VIRREY
25	CHALACO	59	LAGUNA RAMON
26	TALANEO	60	CHIGNIA
27	SAN PEDRO	61	PIRGA
28	PALO BLANCO	62	HUAR HUAR
29	ALTAMIZA	63	PUENTE INTERNACIONAL
30	PALTASHACO	64	CIRUELO
31	PASAPAMA	65	PARAJE GRANDE
32	SAN JOAQUIN	66	LAS LOMAS
33	BARRIOS	67	PAITA
34	BIGOTE	68	HUANCABAMBA

TYPES	NO. OF SYSTEMS
Mesoscale Convective Complex (MCC)	12
Multi-clustered Circular (MC)	33
Multi-clustered Linear (LC)	24
Single-clustered	3
TOTAL	72

Table 2. Number of heavy rainfall producing convective systems.

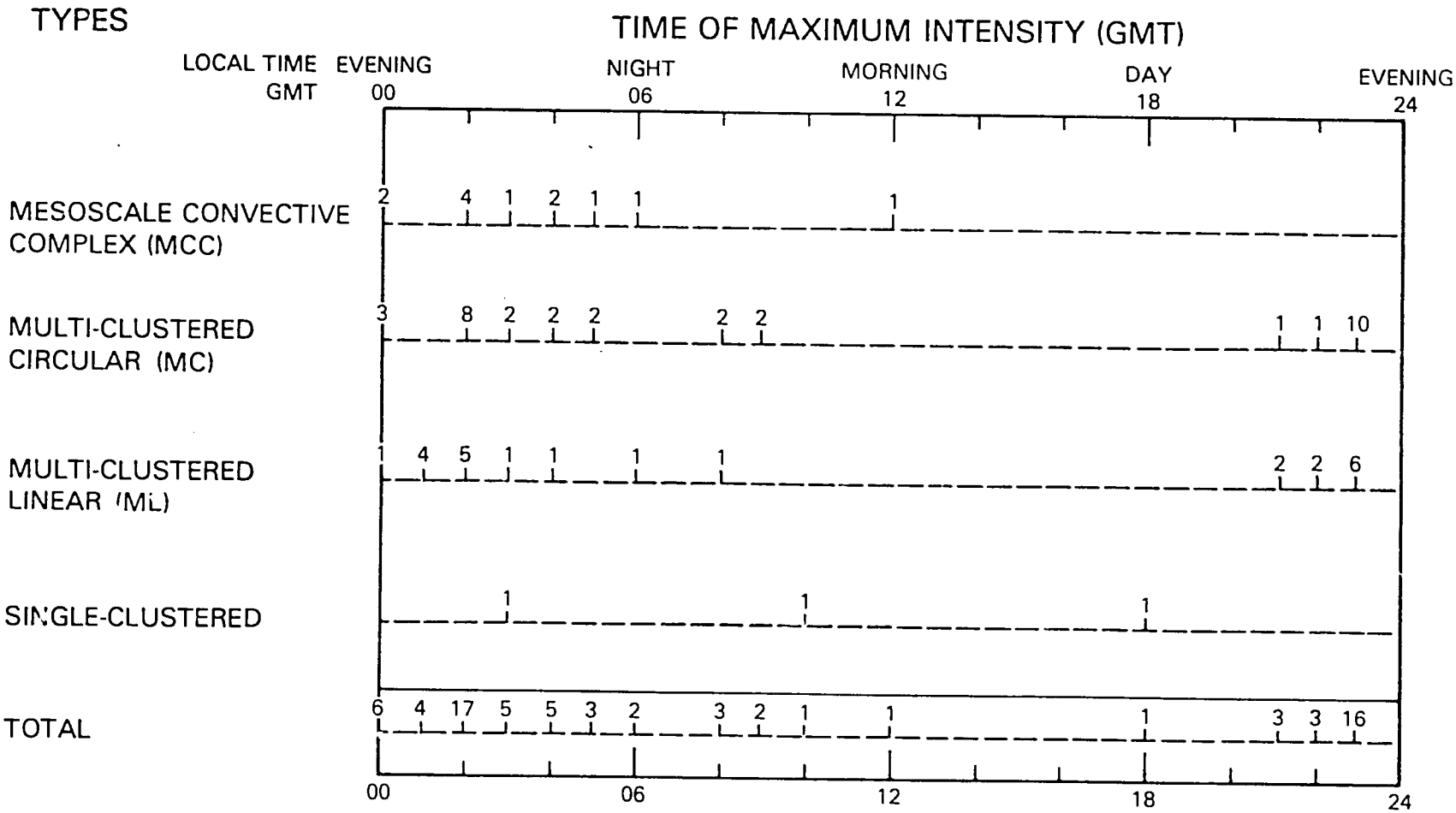

Table 3. Comparison of the observed heavy rainfall producing convective systems to their time of maximum activity.

TYPES	MINIMUM IR CLOUD TOP TEMPERATURE			
	DARK GRAY (WARMER THAN −40°C)	LIGHT GRAY (−40→−60°C)	BLACK (−60→−70°C)	WHITE (COLDER THAN −70°C)
MESOSCALE CONVECTIVE COMPLEX (MCC)	0	0	0	12
MULTI-CLUSTERED CIRCULAR (MC)	0	6	8	19
MULTI-CLUSTERED LINEAR (ML)	0	5	8	11
SINGLE-CLUSTERED	1	1	1	0
TOTAL	1	12	17	42

Table 4. Comparison of the observed heavy rainfall producing convective systems to their minimum infrared cloud top temperatures.

TYPES	MESO-β (~25 ►~250 KM)	MESO-γ (~2.5 ►~25 KM)
MESOSCALE CONVECTIVE COMPLEX (MCC)	12	0
MULTI-CLUSTERED CIRCULAR (MC)	23	10
MULTI-CLUSTERED LINEAR (ML)	15	9
SINGLE-CLUSTERED	0	3
TOTAL	50	22

Table 5. Meteorological scale sizes for the observed heavy rainfall producing convective systems.

TYPES	DURATION OF EVENT-T (HOURS)			
	$0<T<3$	$3\leqslant T<6$	$6\leqslant T<12$	$T\geqslant 12$
MESOSCALE CONVECTIVE COMPLEX (MCC)	0	0	6	6
MULTI-CLUSTERED CIRCULAR (MC)	10	18	4	1
MULTI-CLUSTERED LINEAR (ML)	9	13	2	0
SINGLE-CLUSTERED	2	0	1	0
TOTAL	21	31	13	7

Table 6. Duration of the observed heavy rainfall producing convective systems.

FIGURE CAPTIONS

Figure 1. A) Geographical distribution of the 66 rainfall stations in northwestern Peru used for this study. B) Computer generated relief map based on station altitudes. A cluster of four stations at Chulucanas, San Pedro, Morropon, and Santo Domingo is highlighted and the coastline is marked for reference.

Figure 2. Daily rainfall means (in mm) using all 66 ground stations for the interval November-June. A) Average of 1980-81 and 1981-82 periods. B) 1982-83 (El Niño period). C) Average of 1983-84 and 1984-85 periods.

Figure 3. Daily rainfall means (in mm) using all 66 stations partitioned into 10 altitude sectors, for the interval November-June. A) Average of four non-El Niño periods: 1980-81, 1981-82, 1983-84, 1984-85. B) 1982-83 (El Niño period).

Figure 4. Station map representation of daily rainfall (mm) in northwestern Peru for the period April 3-8, 1983. Station symbols are coded according to daily total rainfall. A four station cluster and the coastline are indicated for reference as in figure 1B.

Figure 5. Contour maps of daily rainfall (mm) in northwestern Peru for the period April 3-8, 1983 based on the data of figure 4. A four station cluster and the coastline are indicated for reference as in figure 1B.

Figure 6. Comparison of unenhanced and enhanced IR GOES photographs of a heavy rainfall producing convective

system over northwestern Peru on January 26, 1983. Panels A, B, and C refer to 0101, 0200, and 0330 GMT, respectively. The enhanced IR temperature key is shown on panel C.

Figure 7. Types of heavy precipitation producing convective systems; thunderstorms are displayed using enhanced IR imagery.

Figure 8. GOES unenhanced and enhanced IR photographs showing the merger (to M) of two thunderstorm clusters (A and B) on April 3, 1983. Panels 1, 2, and 3 depict conditions at 0030, 0300, and 0630 GMT, respectively. Panel 3 also displays rainfall estimates using the NESDIS technique (Scofield, 1987).

Figure 9. Daily total rainfall at Chulucanas for March-April, 1983.

Figure 10. Contours of mean rainfall (A) for a typical non-El Niño year and (B) for the 1983 El Niño year (after Mugica, pvt. communication, 1986).

Figure 11. Photograph of the terrain looking northeast from Chulucanas.

Figure 12. Visible GOES photographs above the Peruvian sector depicting convective cloud line development on April 3, 1983 (panel A) followed by mergers and east-west rain bands over northern Peru on April 4, 1983 (panel B).

Figure 13. Example of convective cloud line merger over the gulf coast of the United States on 15 June 1977, 2000 GMT.

Figure 14. Wind structure over Peru on April 3, 1983. (A) Winds at 700 mb depicting strong easterly flow. (B) Surface wind map demonstrating parallel flow with the Andes and Peruvian coastline.

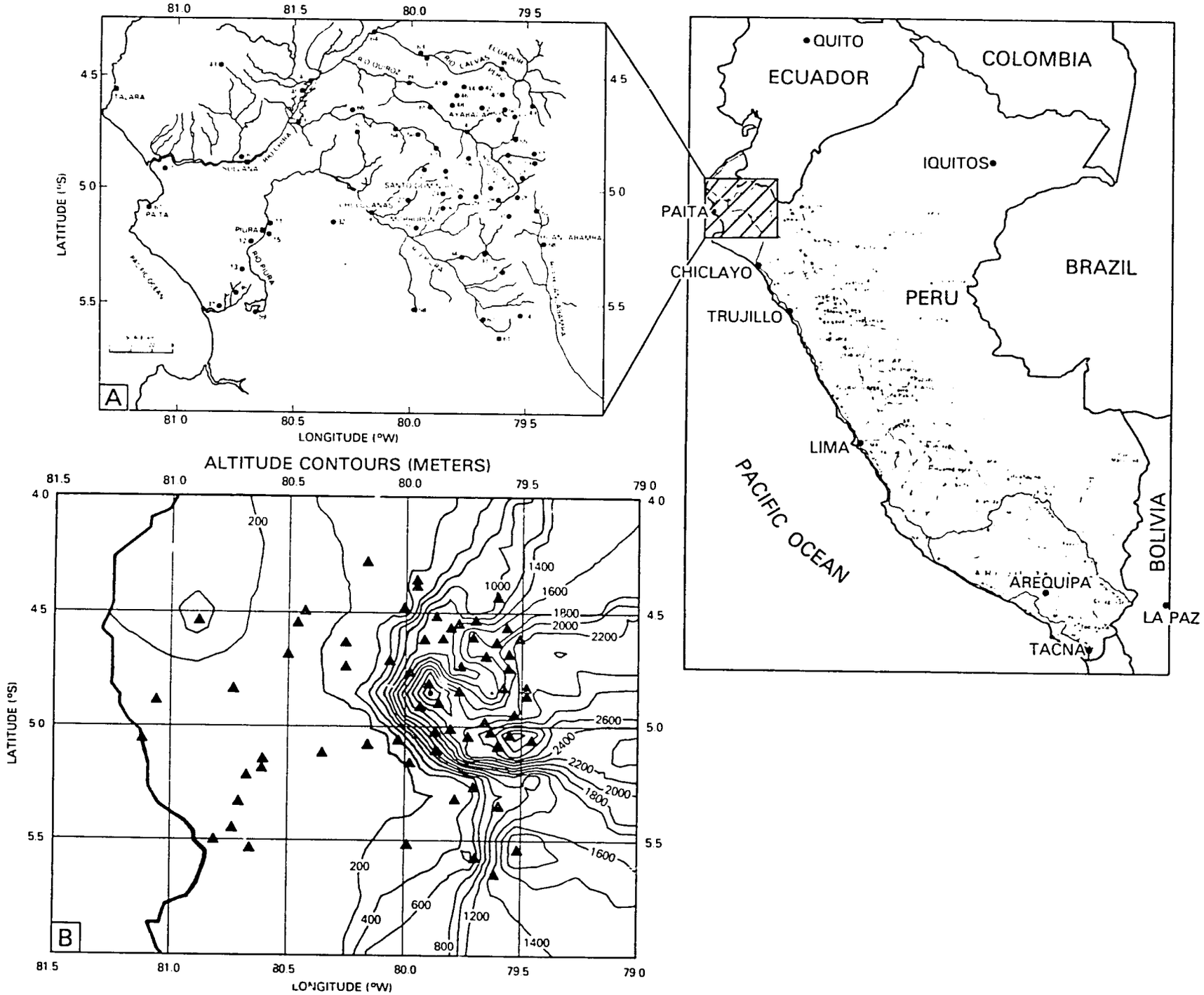
81.0
81.5
80.0
79.5
4.5
5.0
5.5
LATITUDE (°S)
LONGITUDE (°W)
A
B
ALTITUDE CONTOURS (METERS)
200
400
600
800
1000
1200
1400
1600
1800
2000
2200
2400
2600
81.5
81.0
80.5
80.0
79.5
79.0
4.0
4.5
5.0
5.5
LATITUDE (°S)
LONGITUDE (°W)
QUITO
ECUADOR
COLOMBIA
IQUITOS
PAITA
CHICLAYO
TRUJILLO
PERU
BRAZIL
LIMA
PACIFIC OCEAN
AREQUIPA
BOLIVIA
LA PAZ
TACNA

Figure 1

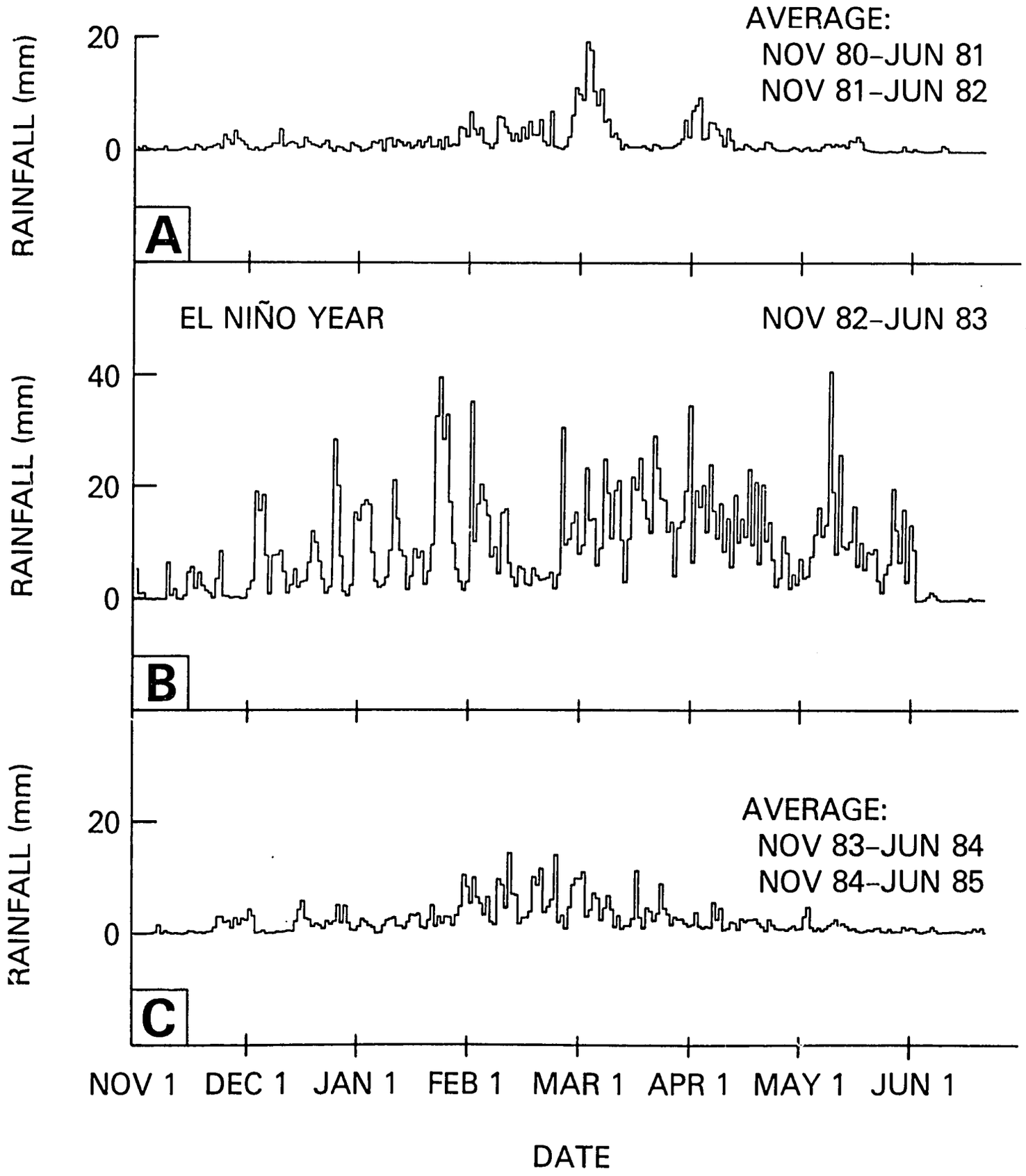
AVERAGE:
NOV 80–JUN 81
NOV 81–JUN 82
RAINFALL (mm)
20
0
A
EL NIÑO YEAR
NOV 82–JUN 83
40
20
0
B
AVERAGE:
NOV 83–JUN 84
NOV 84–JUN 85
20
0
C
NOV 1
DEC 1
JAN 1
FEB 1
MAR 1
APR 1
MAY 1
JUN 1
DATE

Figure 2

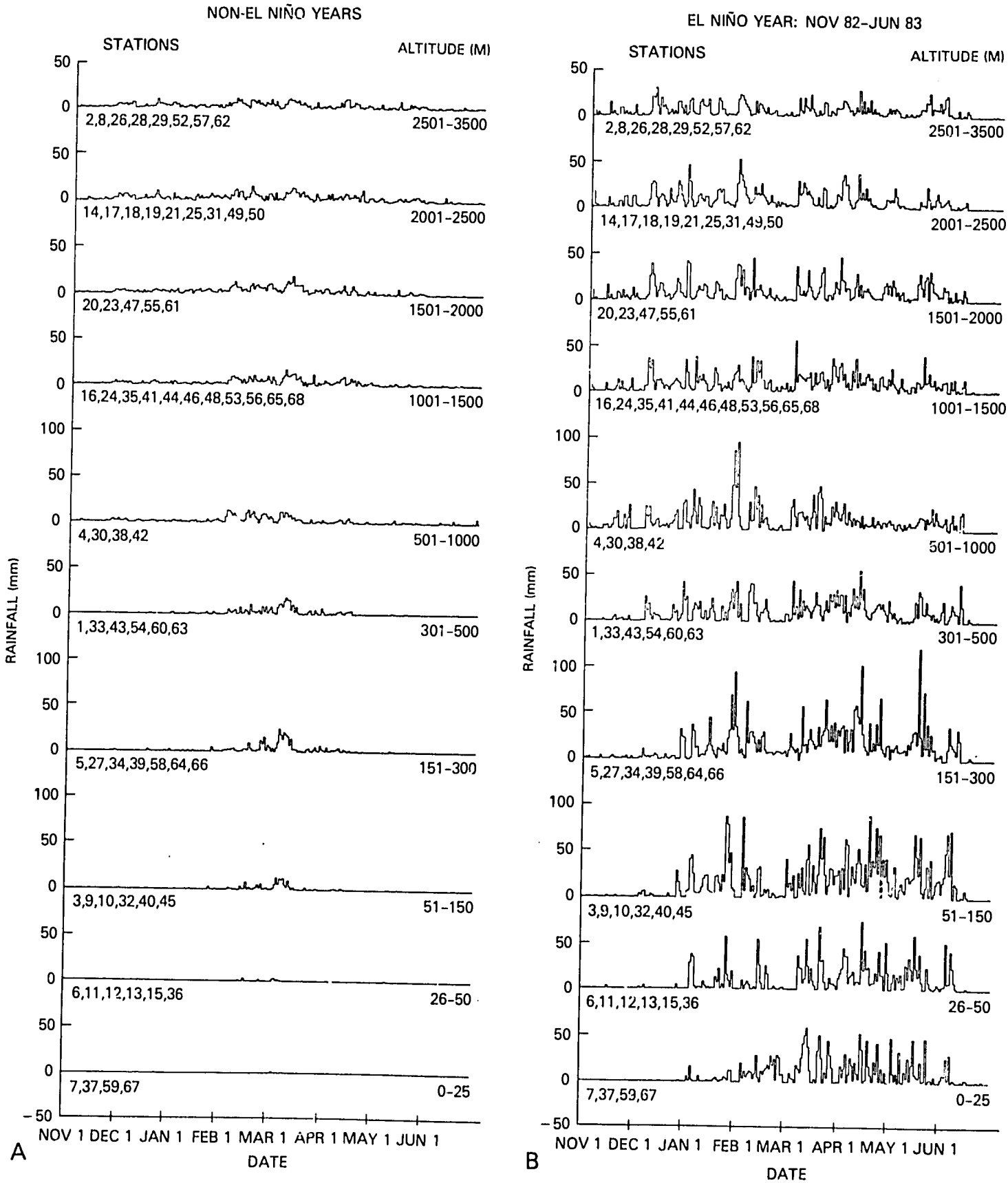
NON-EL NIÑO YEARS
STATIONS
ALTITUDE (M)
2,8,26,28,29,52,57,62
2501-3500
14,17,18,19,21,25,31,49,50
2001-2500
20,23,47,55,61
1501-2000
16,24,35,41,44,46,48,53,56,65,68
1001-1500
4,30,38,42
501-1000
1,33,43,54,60,63
301-500
5,27,34,39,58,64,66
151-300
3,9,10,32,40,45
51-150
6,11,12,13,15,36
26-50
7,37,59,67
0-25
RAINFALL (mm)
NOV 1 DEC 1 JAN 1 FEB 1 MAR 1 APR 1 MAY 1 JUN 1
DATE
A
EL NIÑO YEAR: NOV 82-JUN 83
STATIONS
ALTITUDE (M)
2,8,26,28,29,52,57,62
2501-3500
14,17,18,19,21,25,31,49,50
2001-2500
20,23,47,55,61
1501-2000
16,24,35,41,44,46,48,53,56,65,68
1001-1500
4,30,38,42
501-1000
1,33,43,54,60,63
301-500
5,27,34,39,58,64,66
151-300
3,9,10,32,40,45
51-150
6,11,12,13,15,36
26-50
7,37,59,67
0-25
RAINFALL (mm)
NOV 1 DEC 1 JAN 1 FEB 1 MAR 1 APR 1 MAY 1 JUN 1
DATE
B

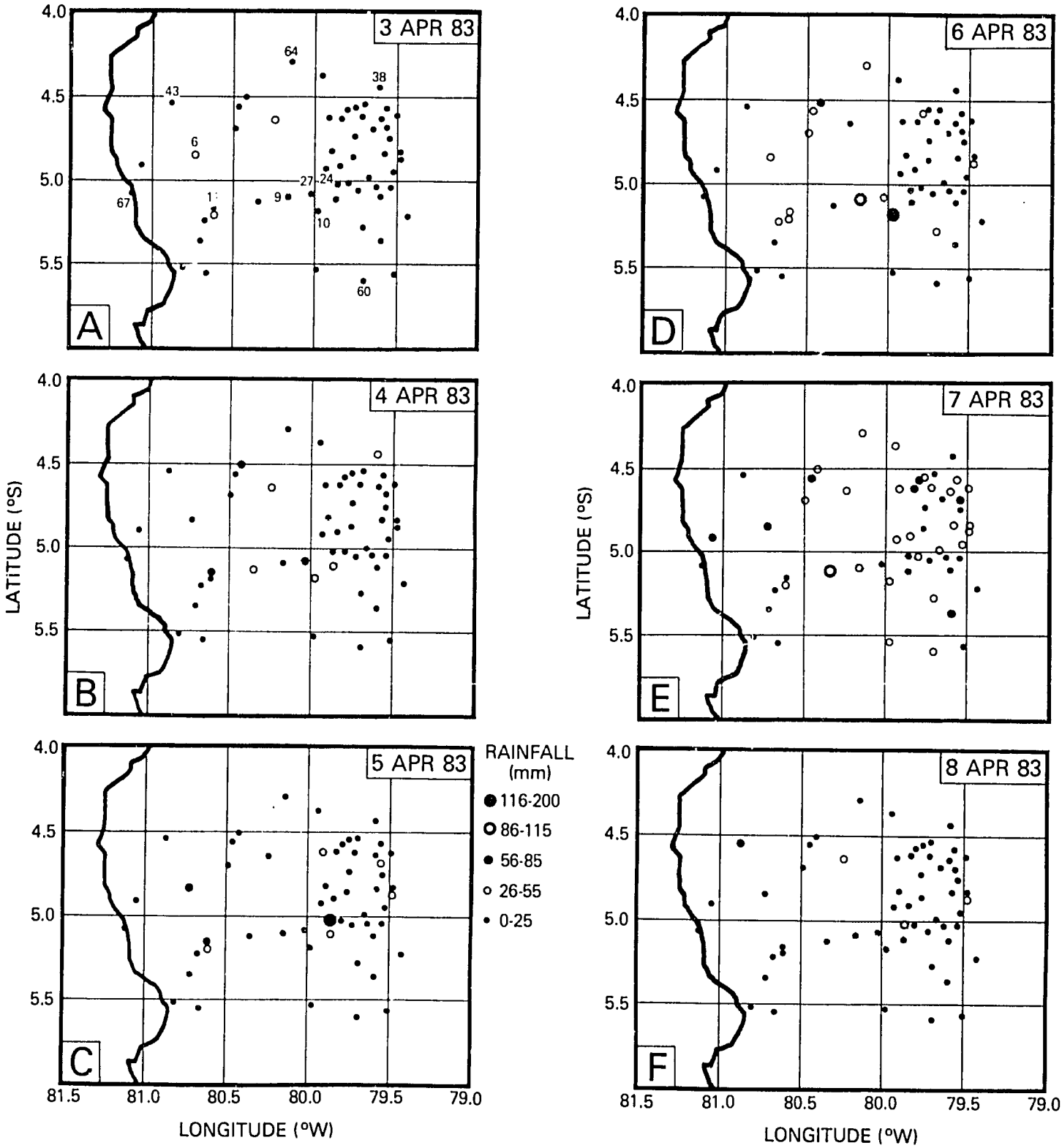
3 APR 83
4 APR 83
5 APR 83
6 APR 83
7 APR 83
8 APR 83
A
B
C
D
E
F
64
38
43
6
27
24
67
9
10
60
4.0
4.5
5.0
5.5
81.5
81.0
80.5
80.0
79.5
79.0
LATITUDE (°S)
LONGITUDE (°W)
RAINFALL (mm)
116-200
86-115
56-85
26-55
0-25

Figure 4

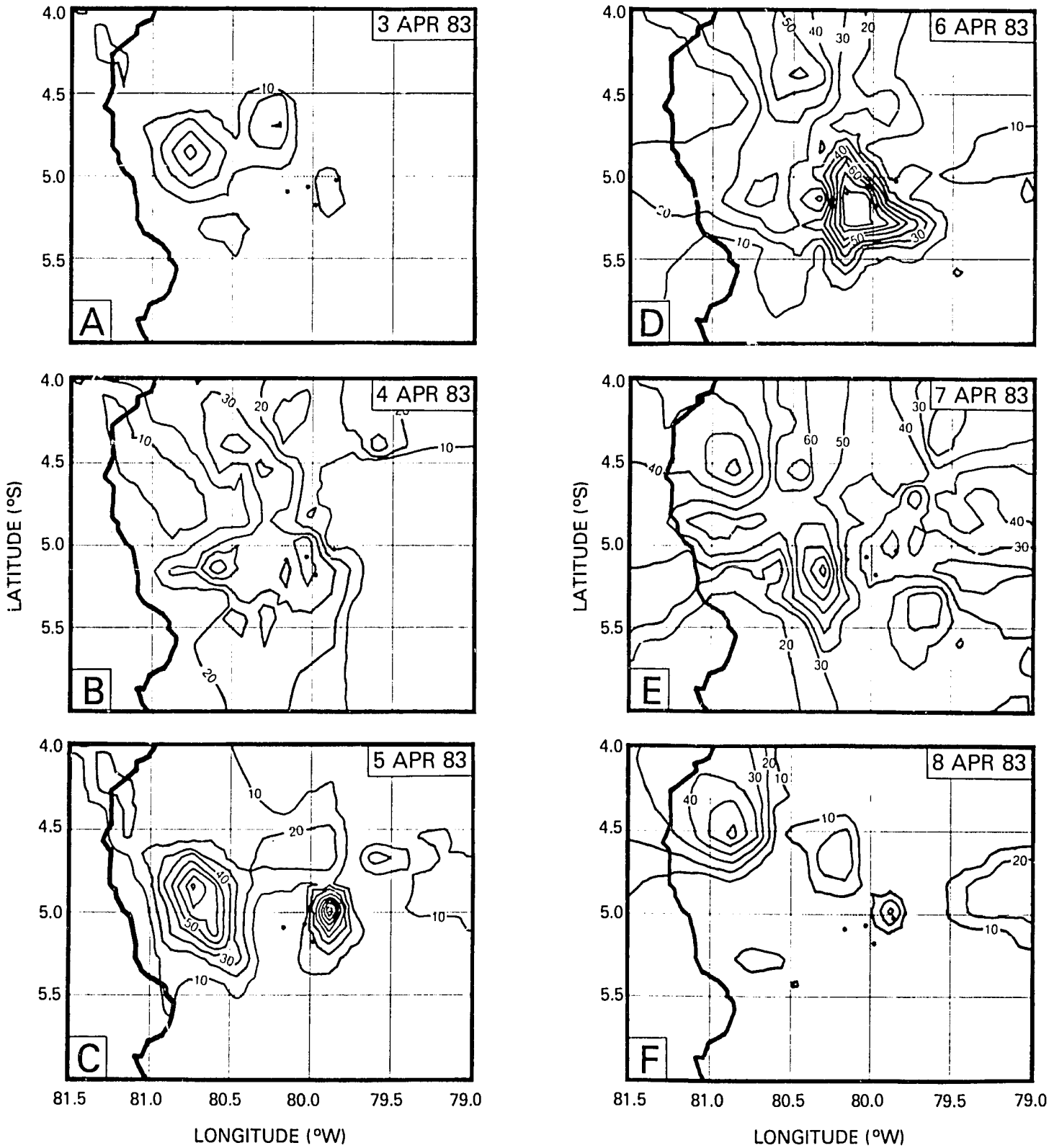
RAINFALL CONTOURS IN MILLIMETERS
3 APR 83
4 APR 83
5 APR 83
6 APR 83
7 APR 83
8 APR 83
A
B
C
D
E
F
LATITUDE (°S)
LONGITUDE (°W)
4.0
4.5
5.0
5.5
81.5
81.0
80.5
80.0
79.5
79.0

Figure 5

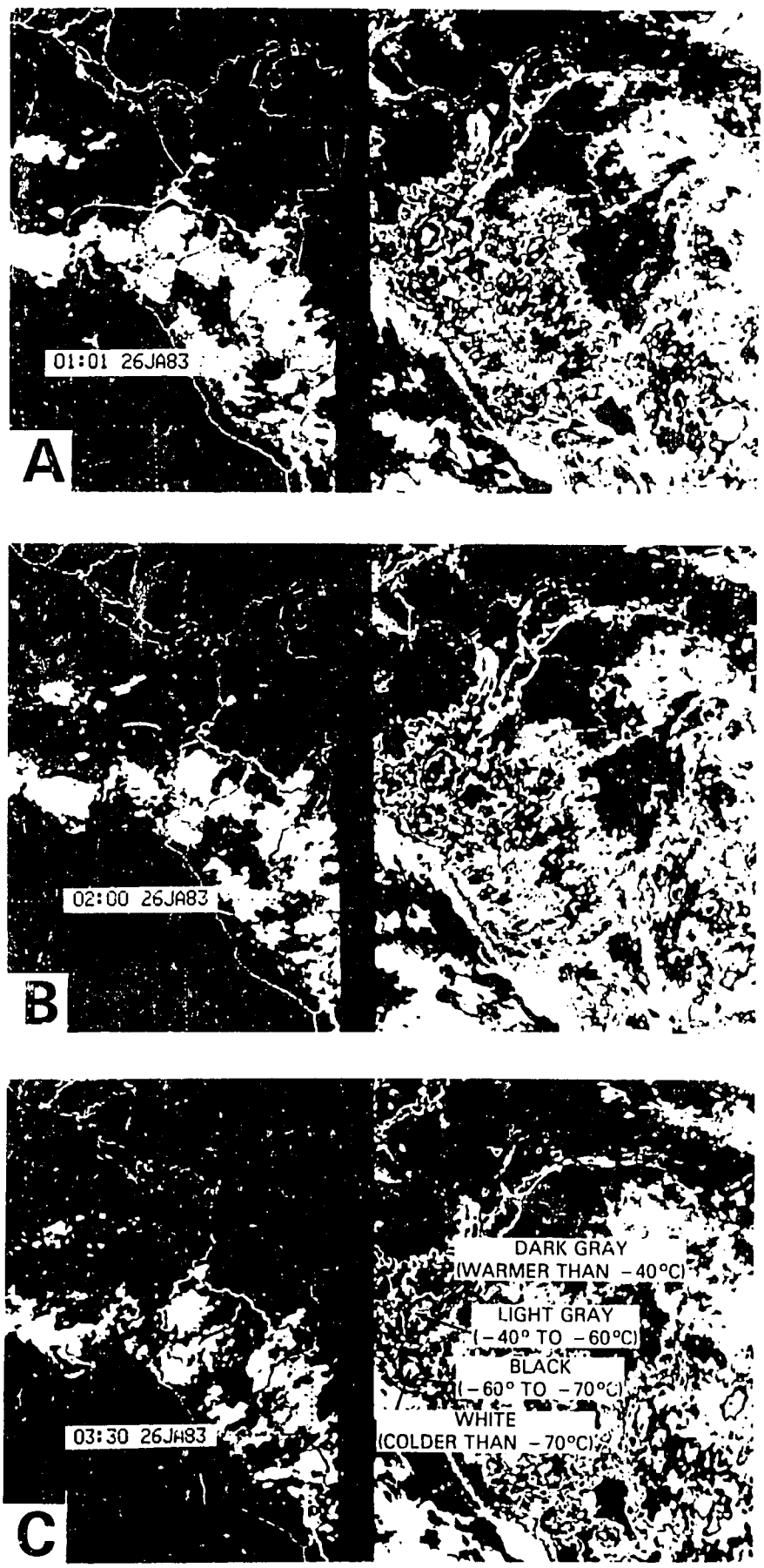
UNENHANCED
ENHANCED
01:01 26JA83
A
02:00 26JA83
B
03:30 26JA83
C
DARK GRAY
(WARMER THAN −40°C)
LIGHT GRAY
(−40° TO −60°C)
BLACK
(−60° TO −70°C)
WHITE
(COLDER THAN −70°C)

Figure 6

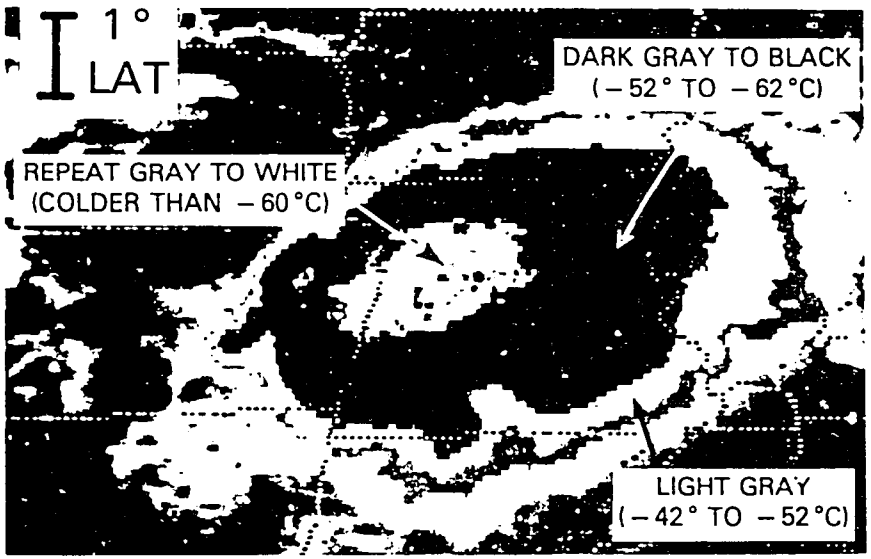

MESOSCALE CONVECTIVE COMPLEX

MULTI-CLUSTERED LINEAR

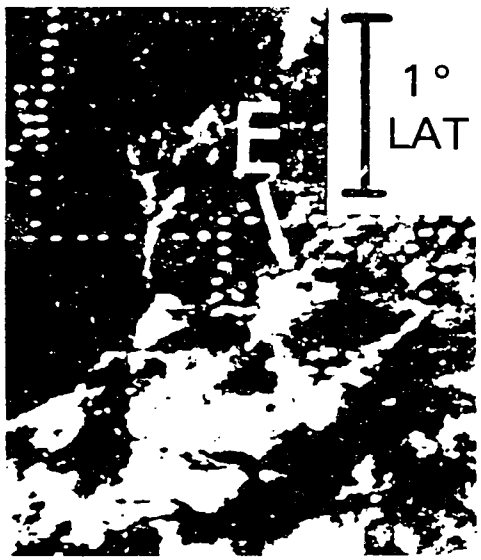

SINGLE-CLUSTERED

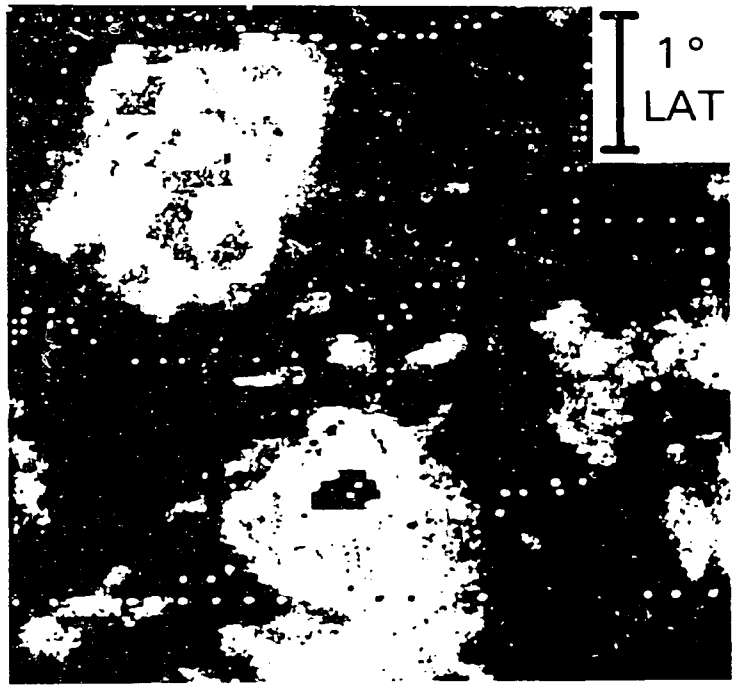

MULTI-CLUSTERED CIRCULAR

Figure

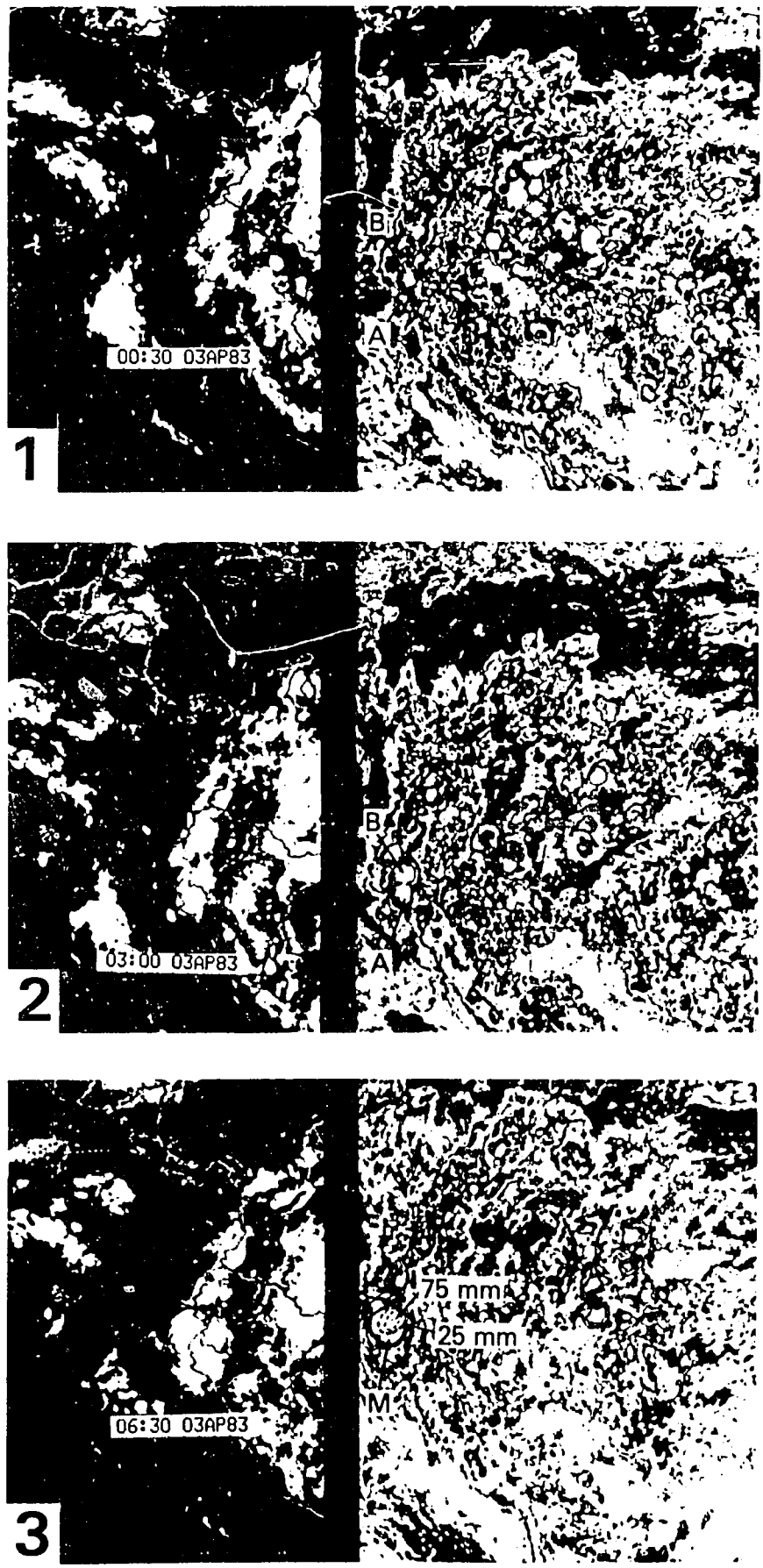
UNENHANCED
ENHANCED
00:30 03AP83
1
B
A
03:00 03AP83
2
B
A
06:30 03AP83
3
75 mm
25 mm
M

Figure 8

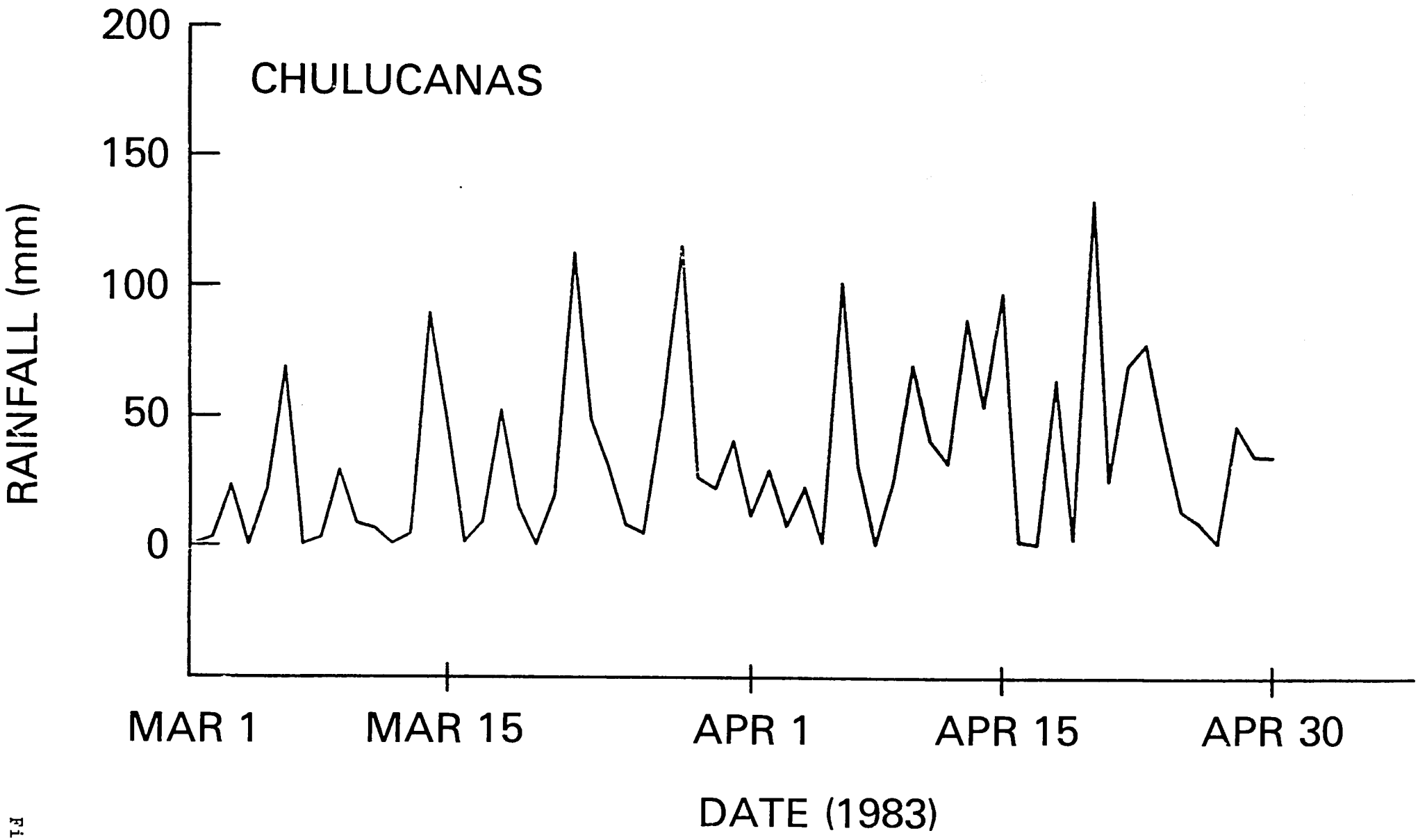
CHULUCANAS
200
150
100
50
0
RAINFALL (mm)
MAR 1
MAR 15
APR 1
APR 15
APR 30
DATE (1983)

Figure 9

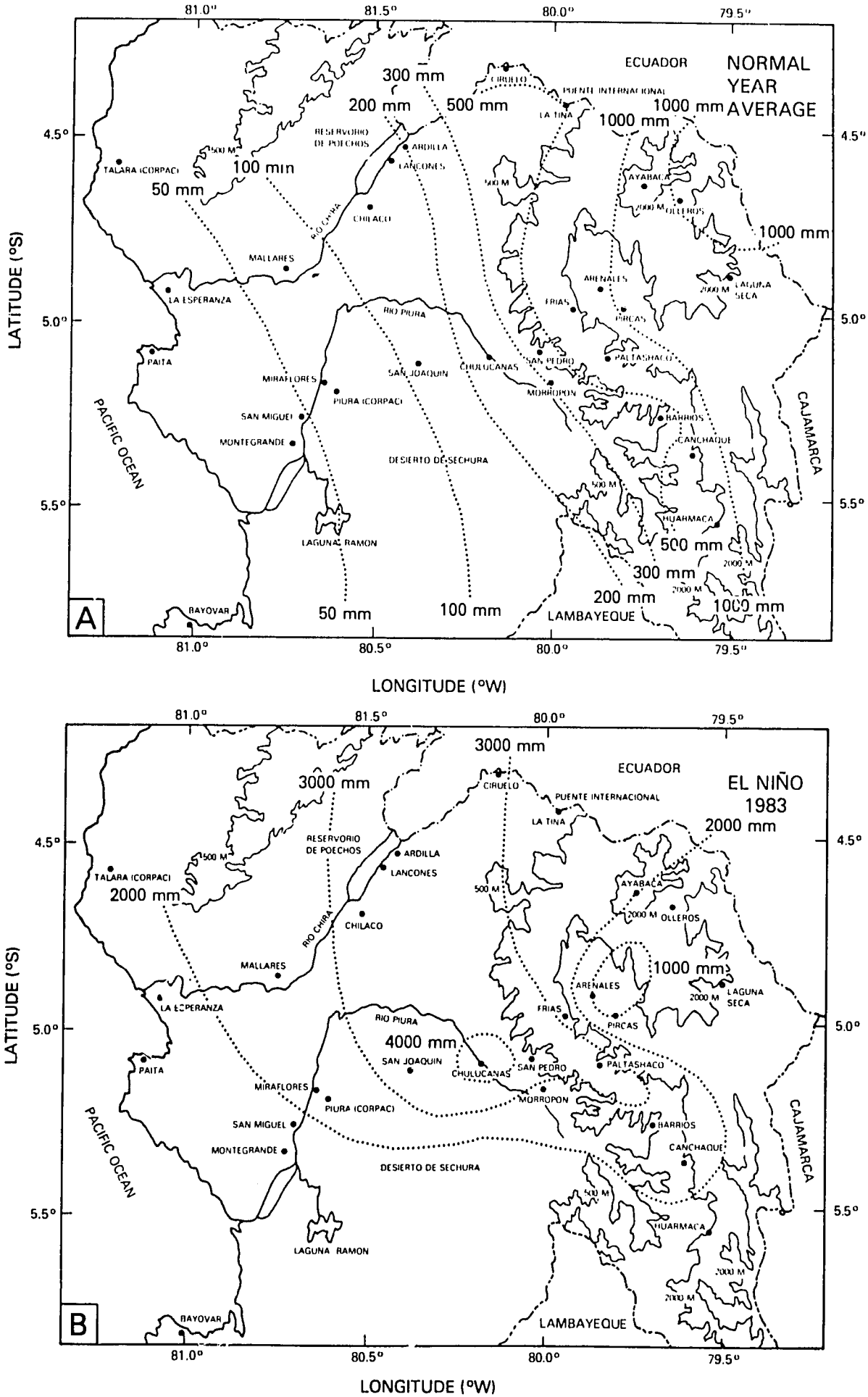
81.0°
81.5°
80.0°
79.5°
ECUADOR
NORMAL YEAR AVERAGE
300 mm
200 mm
500 mm
1000 mm
100 min
50 mm
CIRUELO
PUENTE INTERNACIONAL
LA TINA
RESERVORIO DE POECHOS
ARDILLA
LANCONES
TALARA (CORPAC)
AYABACA
OLLEROS
CHILACO
RIO CHIRA
MALLARES
LA ESPERANZA
ARENALES
LAGUNA SECA
FRIAS
PIRCAS
RIO PIURA
PAITA
SAN JOAQUIN
CHULUCANAS
SAN PEDRO
PALTASHACO
MIRAFLORES
MORROPON
PIURA (CORPAC)
SAN MIGUEL
BARRIOS
CAJAMARCA
MONTEGRANDE
CANCHAQUE
DESIERTO DE SECHURA
PACIFIC OCEAN
HUARMACA
LAGUNA RAMON
A
BAYOVAR
LAMBAYEQUE
4.5°
5.0°
5.5°
LATITUDE (°S)
LONGITUDE (°W)
3000 mm
4000 mm
2000 mm
EL NIÑO 1983
B

Figure 10

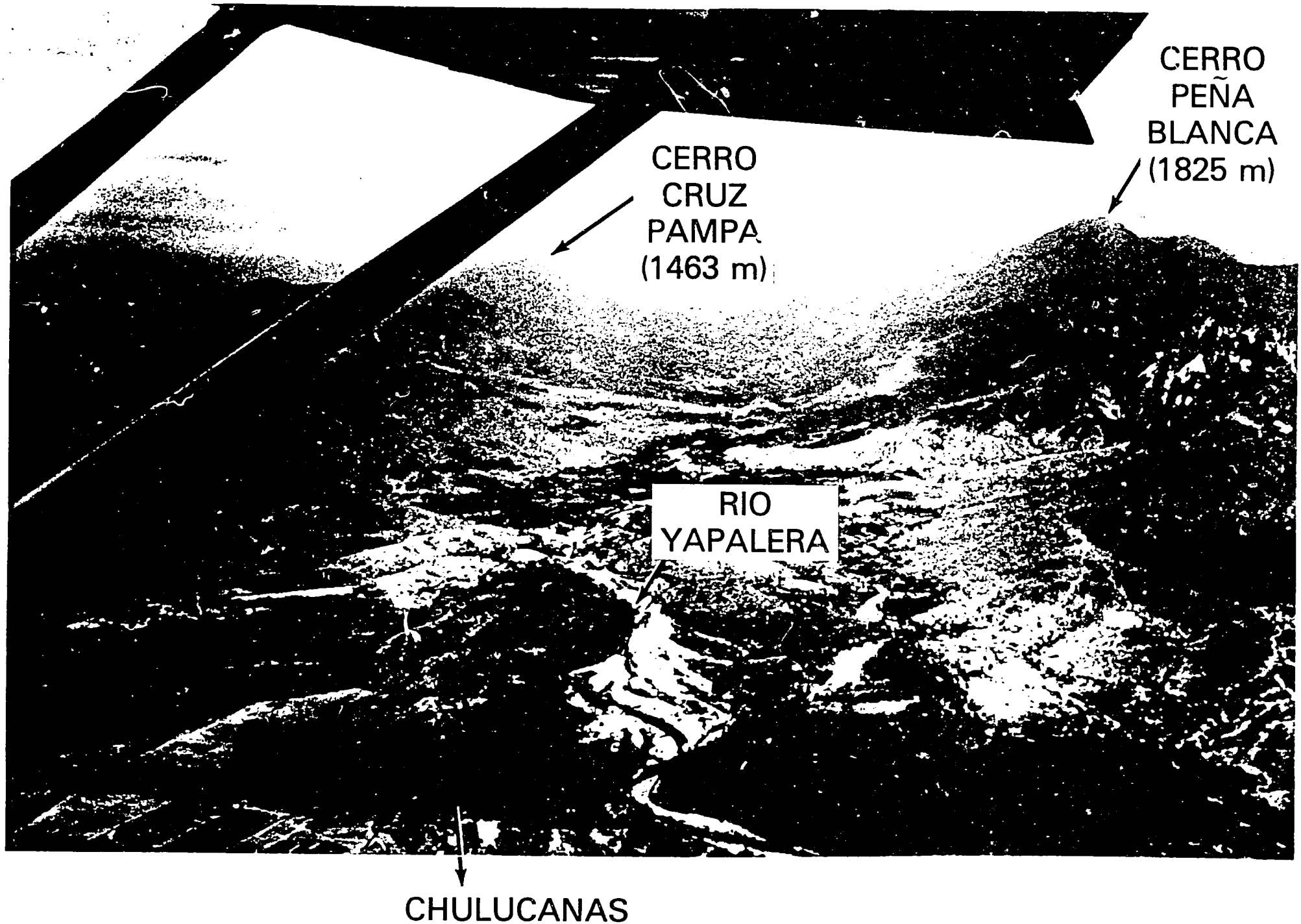
CERRO
PEÑA
BLANCA
(1825 m)
CERRO
CRUZ
PAMPA
(1463 m)
RIO
YAPALERA
CHULUCANAS

Figure 11

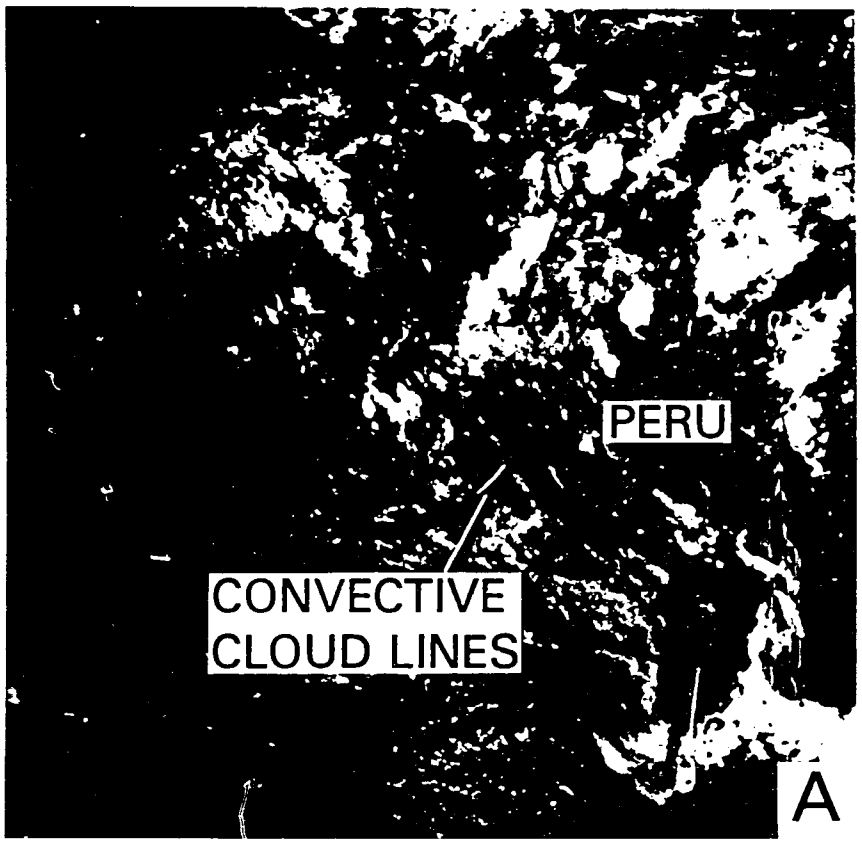

3 APR 83
1500 GMT

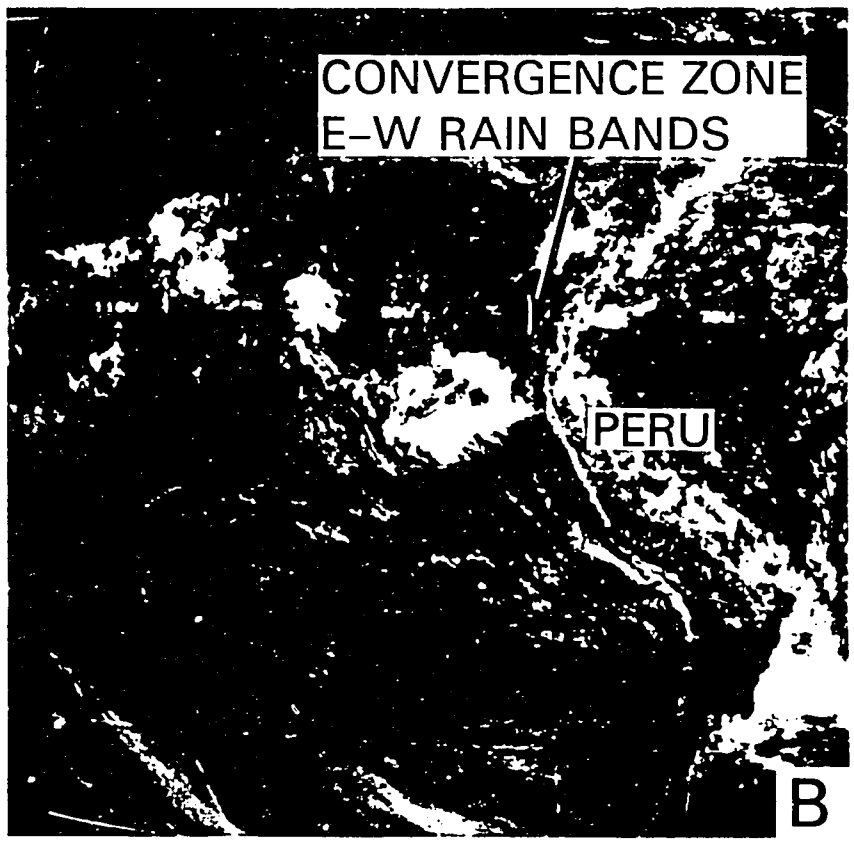

4 APR 83
1800 GMT

Figure 12

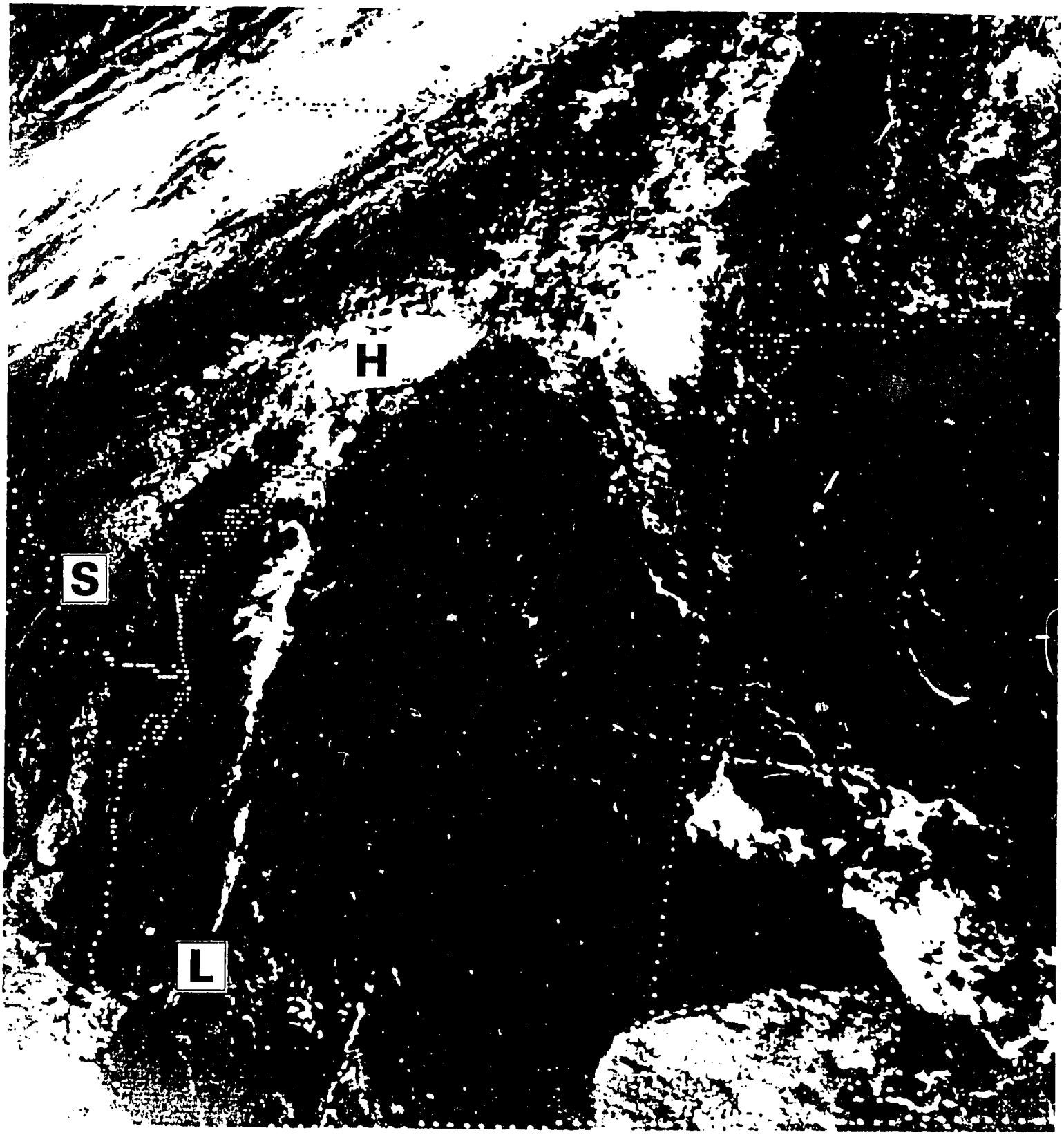

Figure 13

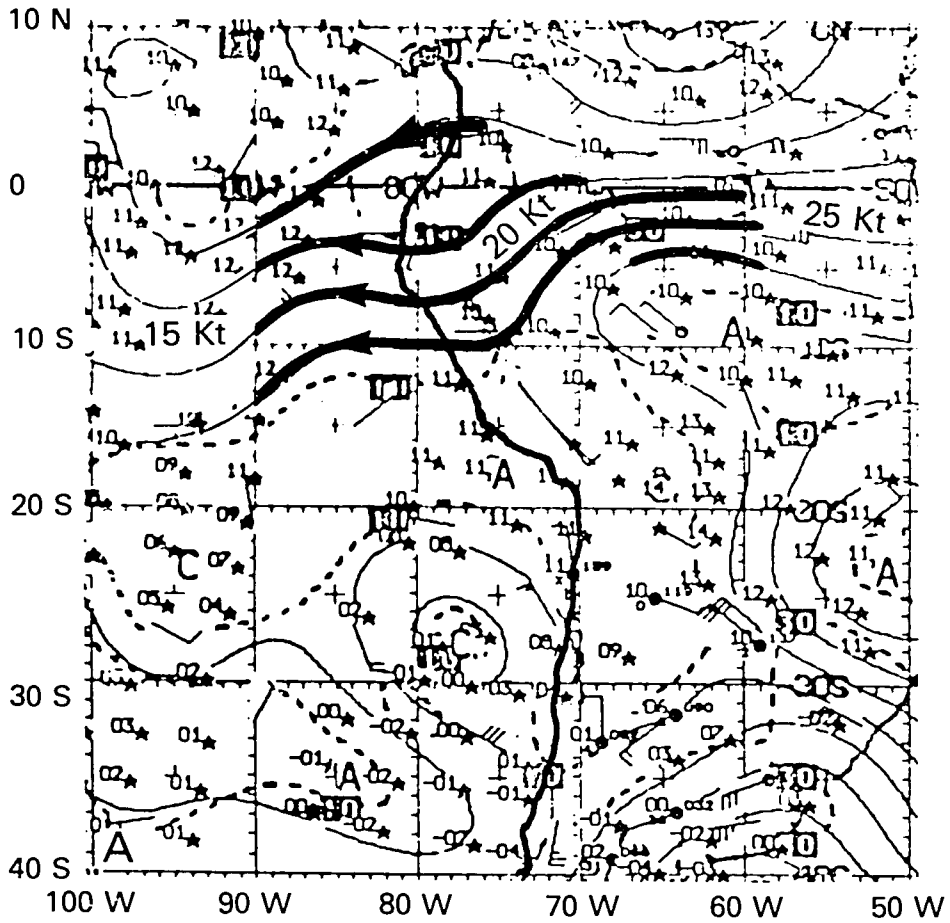

3 APR 83
700 MB
1200 GMT

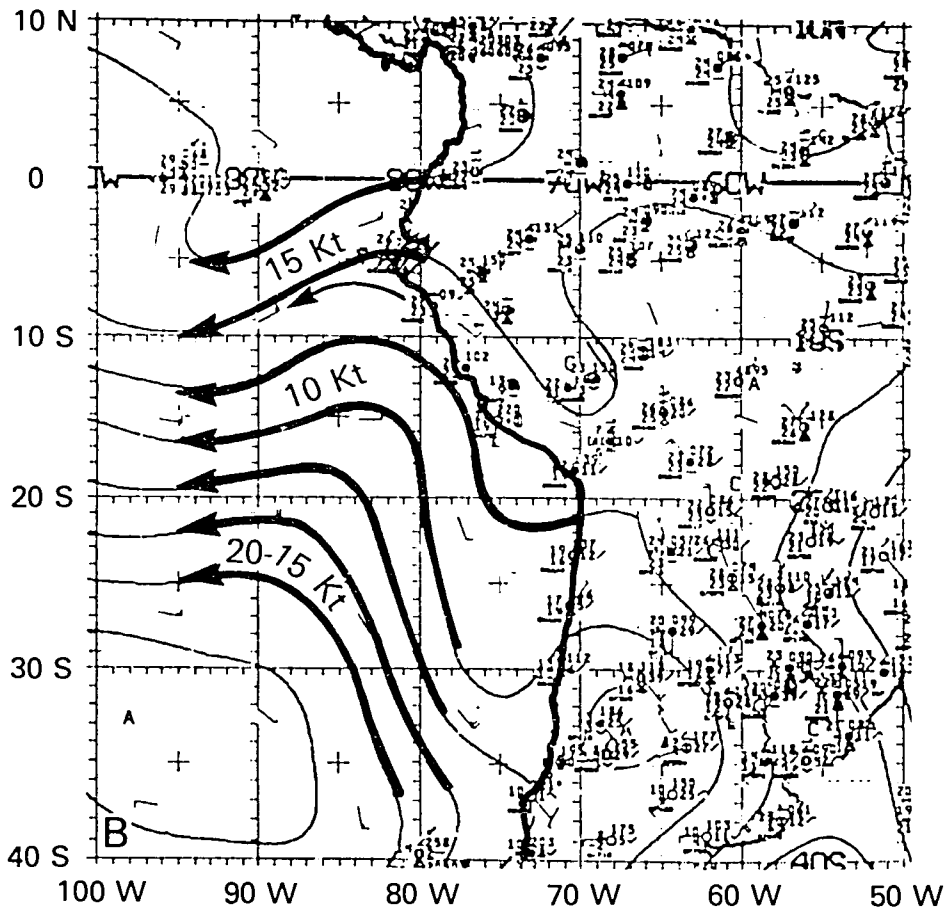

3 APR 83
SURFACE
1200 GMT

Figure 14